Photocatalytic decolorization of Basic Blue 41 using TiO$_2$-Fe$_3$O$_4$-bentonite coating applied to ceramic in continuous system

Restu Kartiko Widi, Inez Suciani, Emma Savitri, Rafael Reynaldi & Arief Budhyantoro

Published online: 21 Feb 2019.

Submit your article to this journal ⍚

View Crossmark data ⍚

Chemical Engineering Communications

Country	United Kingdom - IIII SIR Ranking of United Kingdom

Subject Area and Category	Chemical Engineering
	    Chemical Engineering (miscellaneous)
	
	Chemistry
	    Chemistry (miscellaneous)

Publisher	Taylor & Francis
Publication type	Journals
ISSN	00986445, 15635201
Coverage	1973-1976, 1978-ongoing
Scope	Chemical Engineering Communications provides a forum for the publication of manuscripts reporting on results of both basic and applied research. All conventional areas of chemical engineering will be considered as well as topics in semiconductor processing, materials engineering, bioengineering, fluid mechanics, the molecular theory of equilibrium and transport properties, applied mathematics and computer-aided design.

44

H Index

� Homepage
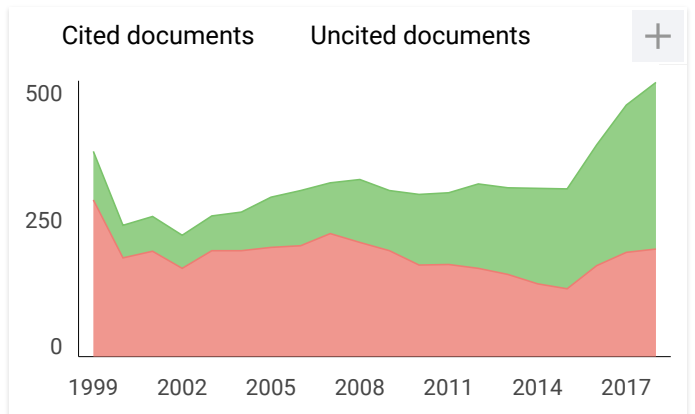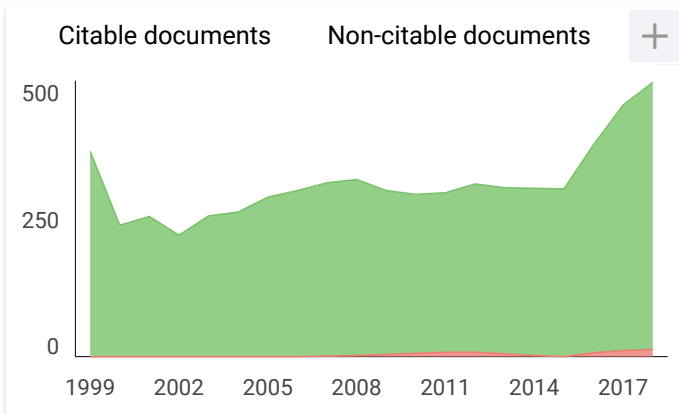
💬 Join the conversation about this journal
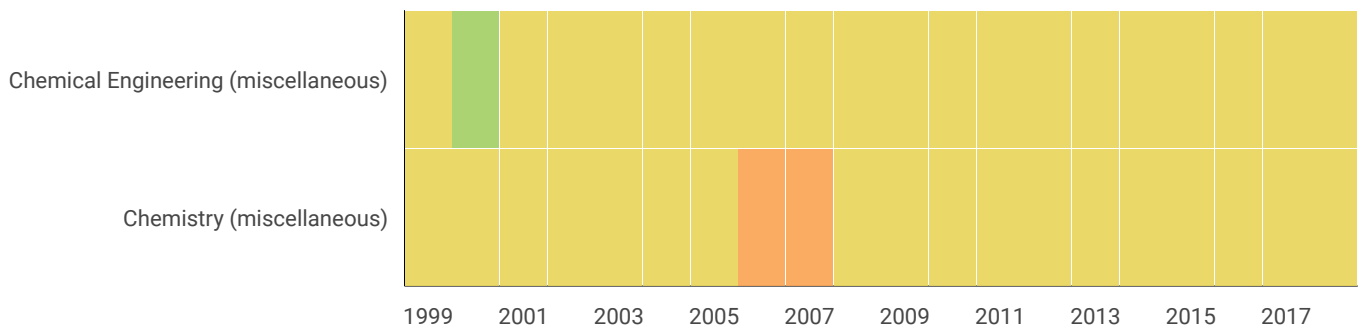
Quartiles

SJR

Citations per document

0.6

Total Cites   Self-Cites   +

1k

500

0

1999 2002 2005 2008 2011 2014 2017

1.8

1.5

1.2

0.9

0.6

0.3

External Cites per Doc   Cites per Doc   +

2.1

1.4

0.7

0

1999 2002 2005 2008 2011 2014 2017

% International Collaboration   +

40

20

0

1999 2002 2005 2008 2011 2014 2017

Citable documents   Non-citable documents   +

500

250

0

1999 2002 2005 2008 2011 2014 2017

Cited documents   Uncited documents   +

500

250

0

1999 2002 2005 2008 2011 2014 2017

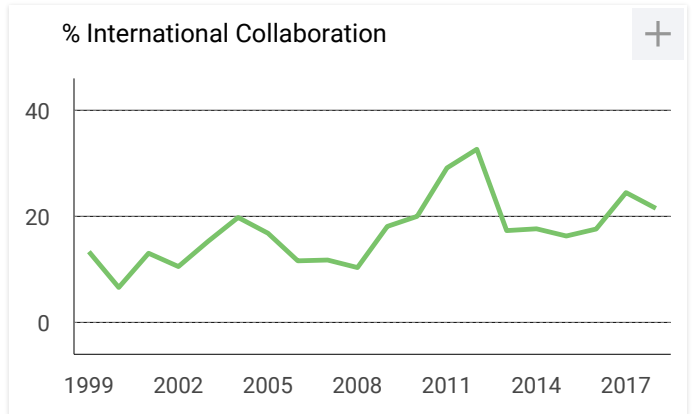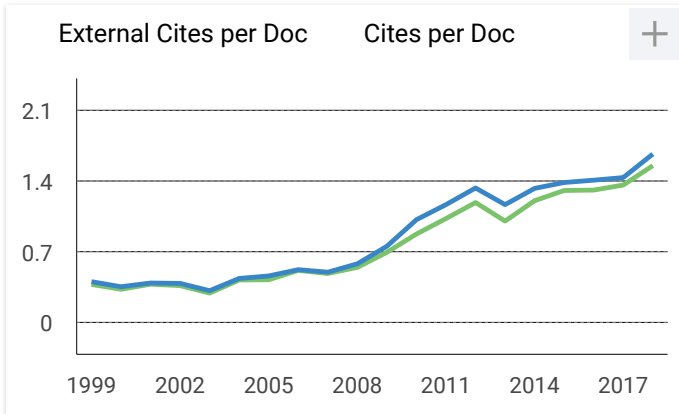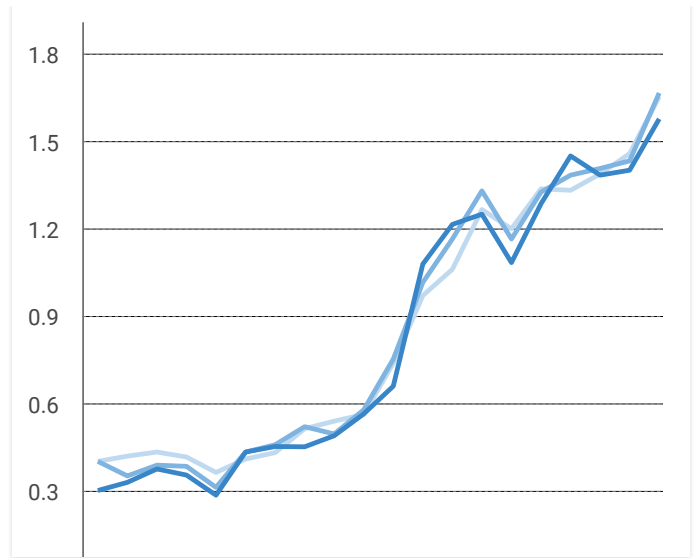**Chemical Engineering Communications**

Q2 | Chemical Engineering (miscellaneous)
best quartile

SJR 2018
0.38

powered by scimagojr.com

← Show this widget in your own website

Just copy the code below and paste within your html code:

`<a href="https://www.scimag`

Leave a comment

Source details

Chemical Engineering Communications

Scopus coverage years: from 1973 to 1976, from 1978 to Present

Publisher: Taylor & Francis

ISSN: 0098-6445 E-ISSN: 1563-5201

Subject area: (Chemical Engineering: General Chemical Engineering) (Chemistry: General Chemistry)

View all documents ›   Set document alert   Journal Homepage

CiteScore 2018
1.62 ⓘ
Add CiteScore to your site

SJR 2018
0.375 ⓘ

SNIP 2018
0.680 ⓘ

CiteScore   CiteScore rank & trend   CiteScore presets   Scopus content coverage

CiteScore 2018 ⌄   Calculated using data from 30 April, 2019

$$1.62 = \frac{\text{Citation Count 2018}}{\text{Documents 2015 - 2017*}} = \frac{803 \text{ Citations} ›}{497 \text{ Documents} ›}$$

*CiteScore includes all available document types

View CiteScore methodology ›   CiteScore FAQ ›

CiteScoreTracker 2019 ⓘ   Last updated on *12 August, 2019*
Updated monthly

$$1.28 = \frac{\text{Citation Count 2019}}{\text{Documents 2016 - 2018}} = \frac{580 \text{ Citations to date} ›}{454 \text{ Documents to date} ›}$$

CiteScore rank ⓘ

Category	Rank	Percentile
Chemical Engineering └ General Chemical Engineering	#106/272	61st
Chemistry └ General Chemistry	#162/371	56th

View CiteScore trends ›

Metrics displaying this icon are compiled according to Snowball Metrics ↗ , a collaboration between industry and academia.

About Scopus

What is Scopus
Content coverage
Scopus blog
Scopus API
Privacy matters

Language

日本語に切り替える
切換到简体中文
切換到繁體中文
Русский язык

Customer Service

Help
Contact us

This journal

- › Aims and scope
- › Instructions for authors
- › Journal information
- › Editorial board
- › Related websites

Editorial board

Articles

Photocatalytic decolorization of Basic Blue 41 using TiO$_2$-Fe$_3$O$_4$-bentonite coating applied to ceramic in continuous system

Restu Kartiko Widi ✉, Inez Suciani, Emma Savitri, Rafael Reynaldi & Arief Budhyantoro
Published online: 21 Feb 2019

📄 Full Article   🖼 Figures & data   📖 References   ❝ Citations   📊 Metrics   🖨 Reprints & Permissions   Get access

Abstract

Photocatalytic degradation/decolorization of Basic Blue 41 dye assisted by UV radiation has been studied over TiO$_2$-Fe$_3$O$_4$ supported by bentonite. In this experiment, photocatalytic decolorization process was performed continuously; where dye feed solution was supplied to a coated-ceramic vessel. The influence of the initial concentration, pH, and flow rate of the dye feed solution on the degradation efficiency process was examined in this study. The results showed that the increase in the dye concentration and flow rate reduces decolorization efficiency. The highest decolorization efficiency was at pH of 5.5. The kinetic study of this photo-decolorization indicated that under the experimental condition, the photocatalytic kinetic process followed first-order kinetics on the basis of Langmuir–Hinshelwood heterogeneous reaction mechanism, where the reaction rate constant, namely k_r, is 0.7707 and the adsorption rate constant, namely K, is 0.01298.

Keywords: Basic Blue 41, Bentonite, Decolorization, Fe$_3$O$_4$, Photocatalytic, TiO$_2$

Taylor & Francis
Taylor & Francis Group

Photocatalytic decolorization of Basic Blue 41 using TiO$_2$-Fe$_3$O$_4$-bentonite coating applied to ceramic in continuous system

Restu Kartiko Widi, Inez Suciani, Emma Savitri, Rafael Reynaldi, and Arief Budhyantoro

Department of Chemical Engineering, University of Surabaya (UBAYA), Surabaya, Indonesia

ABSTRACT

Photocatalytic degradation/decolorization of Basic Blue 41 dye assisted by UV radiation has been studied over TiO$_2$-Fe$_3$O$_4$ supported by bentonite. In this experiment, photocatalytic decolorization process was performed continuously; where dye feed solution was supplied to a coated-ceramic vessel. The influence of the initial concentration, pH, and flow rate of the dye feed solution on the degradation efficiency process was examined in this study. The results showed that the increase in the dye concentration and flow rate reduces decolorization efficiency. The highest decolorization efficiency was at pH of 5.5. The kinetic study of this photo-decolorization indicated that under the experimental condition, the photocatalytic kinetic process followed first-order kinetics on the basis of Langmuir–Hinshelwood heterogeneous reaction mechanism, where the reaction rate constant, namely k_r, is 0.7707 and the adsorption rate constant, namely K, is 0.01298.

Introduction

Most countries are required to setup an effective strategy in developing the industry as the backbone of the economy. Basically, in the midst of this sector, a concept of sustainable development needs to be considered, in which the strategy is focused on meeting the current needs of the sustainability and health of the natural environment (Habib et al., 2012; Widi et al., 2017). Industrial activity, such as textile industries, often produces waste plant in which its presence can harm the environment. In these circumstances, the textile and the dying industries are often blamed for generating a lot of waste causing serious environmental problems (Habib et al., 2012).

Extensive researches are being carried out worldwide to degrade organic pollutants, such as dyes so that they can be discharged to the environment in accordance with the standards of quality (Ameta et al., 2013). In physical purification by adsorption, coagulation and filtration membrane is a physical method which is quite good in the decolorization of dyes (Pignatello et al., 2007; Ahmad and Kumar, 2010; Ai et al., 2010), but the system and the material used are still quite expensive. In addition to its use, these methods still have to consider how to dispose of the pollutants that had been absorbed into the adsorbent (Bhatia et al., 2009).

From some of the dye decolorization processes, an alternative method called a photocatalyst method appears. One type of photocatalyst material widely used for wastewater treatment is TiO$_2$. This is due to its strong oxidizing properties, super-hydrophilicity, and chemical stability (Chanathaworn et al., 2014; Djellabi et al., 2014; Nakata and Fujishima 2012). The effectiveness of TiO$_2$ photocatalytic activity depends on the adsorption capacity (Don et al., 2015). For the purpose of enhancing the adsorption ability, some researchers have immobilized TiO$_2$ or other metal oxides on porous materials (Widi et al., 2014). Several methods of TiO$_2$/clay composite synthesis have been developed through the pillaring process of TiO$_2$ particles either on the surface or into interlayer of the clays to produce dispersed TiO$_2$ (Liu et al.,
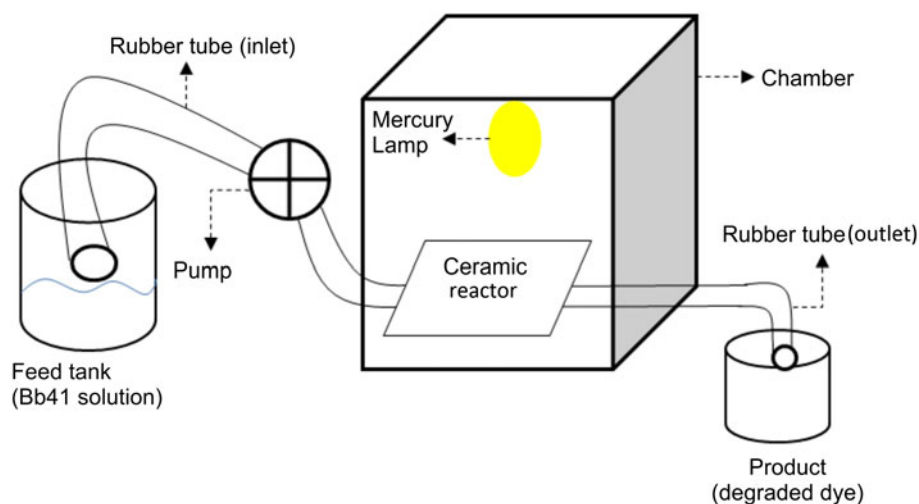
Figure 1. Illustration of experimental setup for continuous photocatalytic reactor.

2007; Judit et al., 2008; Chong et al., 2009; Kameshima et al., 2009; Mahalakshmi et al., 2009; Xie Chen and Dai, 2009; Hadjltaief et al., 2014; Widi and Budhyantoro, 2014; Widi et al., 2015; Hadjltaief et al., 2016).

In the present work, the photocatalyst material was prepared by mixing TiO_2 and Fe_3O_4 and then immobilized using bentonite. The existence of Fe_3O_4 may improve the efficiency of the TiO_2 photocatalytic performance (Savitri et al., 2015). TiO_2 and Fe_3O_4-bentonite were synthesized using Ca-bentonite impregnated with TiO_2-Fe_3O_4 followed by calcination. The material was then coated to the ceramic vessel. XRD and SEM–EDX were used to determine the psychochemical properties of the catalyst, while its photocatalytic activity was tested using a Basic Blue 41 solution under UV irradiation through a continuous system. Basic blue 41 was used as an experiment dye as it is widely used in Indonesian textile industry and cannot be rapidly degradated. Dyes feed solution was supplied to the coated-ceramic vessel.

Experimental

Preparation of TiO_2-Fe_3O_4-bentonite powder

The TiO_2-Fe_3O_4-bentonite powder was synthesized by sol–gel method. The material was prepared by mixing colloidal Ti (from $TiCl_4$) and colloidal Fe (from $FeCl_2{\cdot}4H_2O$ and $FeCl_3{\cdot}6H_2O$), using a ratio of 1:3. Then, these colloids were mixed with bentonite suspension and stirred for

24 h while heated at $50\,°C$. The obtained solid was dried and calcined at $500\,°C$ for 6 h with N_2 and O_2 (4:1 by volume) gas streaming.

The reactor was prepared using the ceramic material with cubic dimensions of $24 \times 19 \times 4\,cm$. The photocatalyst powder was exhaled on the surface of the inside painted-walls of the reactor.

Characterization of materials

X-Ray diffraction analysis was used to characterize the photocatalyst, whereas scanning electron microscope with energy dispersive X-ray analysis (SEM-EDX) was used to characterize the morphology of samples and its specific surface areas. The absorbance of Basic Blue 41 solution was recorded using UV–Vis spectrophotometer with the maximum absorbance wavelength (λ_{max}) was 610 nm.

Experimental setup for continuous and batch photocatalytic reactor

The decolorization of Basic Blue 41 was performed using the TiO_2-Fe_3O_4-bentonite coating on ceramic cube reactor (see "Preparation of TiO_2-Fe_3O_4-bentonite powder" section) under UV high-pressure mercury lamp irradiation. The reactor is placed in the center of the box and irradiated using UV high-pressure mercury light with an intensity of $100\,Watt/m^2$. This intensity is typical value for photocatalytic degradation of basic dye (Zhang et al., 2012). Additionally, the

spectrum of UV high-pressure mercury light is quite similar to the solar spectrum. This is very important to consider, because the application of this degradation technique is expected to work well using solar light. The dye solution was continuously streamed by a pump to the ceramic reactor. The experimental setup for continuous decolorization process was illustrated in Figure 1.

Batch system is used in order to measure the kinetics of decolorization process. The reactor setup is as same as for the continuous system without stirring. For this system, during the mercury irradiation, dye solution was taken from the ceramic reactor every 10 min until getting a clear solution. The concentration of dye solution during reaction process was measured by UV–vis spectrophotometer. The efficiency of degradation process of Basic Blue 41 was defined as by Equation (1) as follows:

$$X_A = \left(\frac{C_{Ao} - C_A}{C_{Ao}}\right) \times 100 \qquad (1)$$

where X_A is the efficiency (%), C_{Ao} is the initial dye concentration (ppm) and C_A is the dye concentration at time t (ppm). From Equation (1), efficiency (%) indicates the conversion value of dye decolorization process.

Result and discussion

Characterization

XRD analysis

From Figure 2 (red line), it can be observed that the characteristic peak of magnetite phase at $2\theta = 35.73°$ and TiO$_2$ anatase phase at $2\theta = 26.59°$ and 30.31° were shown in XRD pattern. The intensity of the magnetite phase is higher than that of TiO$_2$ due to the dominant ratio in material preparation is Fe$_3$O$_4$. The existence of magnetite can control the formation of TiO$_2$ anatase phase, which is able to enhance the photocatalyst process. The emergence of the peak of TiO$_2$ anatase structure shows the formation of anatase crystals in the bentonite. This suggests a relatively easy TiO$_2$ oxide is formed on the surface of bentonite. Figure 2 (black line) depicts the XRD pattern of the photocatalyst material after its performance examination in basic blue photodegradation. From this figure, it can be observed
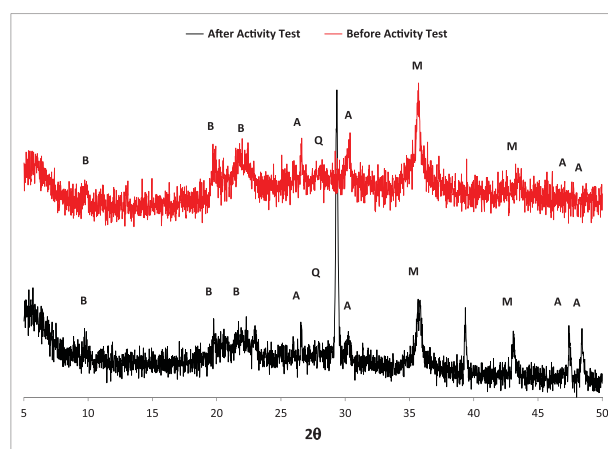

Figure 2. XRD diffractogram of bentonite TiO$_2$–Fe$_3$O$_4$ before (red line) and after (black line) used in photocatalytic performance test.

that the intensity of the anatase and magnetite phase slightly decreased, indicating that some of the catalyst material escaped during the activity test.

However, the emergence high intensity of the peak at $2\theta = 29.37°$ indicates the dominance of the quartz phase in the material. This phenomenon confirms that the anatase and magnetite escape from the vessel during the photocatalytic performance test so that the material bearers of bentonite (in this case the quartz crystals) become more prominent.

SEM-EDX analysis

The morphology of the bentonite-TiO$_2$-Fe$_3$O$_4$ photocatalysts before (Figure 3(a)) and after (Figure 4) used in photocatalytic were studied by the microscope images. A panoramic image of photocatalyst before used in photocatalytic demonstrates that the metal oxides (TiO$_2$ and Fe$_3$O$_4$) are distributed on the bentonite surface with length and width ranging from 0.1 to 3 m. Figure 4 depicts that after photocatalyst used in the photocatalytic process, the material surface noticeably more uniform than before used. This indicates that the material bearers of bentonite covered by the dye Basic Blue as a result of their activities dye adsorption. In addition, TiO$_2$ and Fe$_3$O$_4$ are more distributed on the surface after used. Additionally, it is believed that the catalyst material was reduced from the container after used. This probably because of a container that has been used many times in photocatalytic cause the photocatalyst
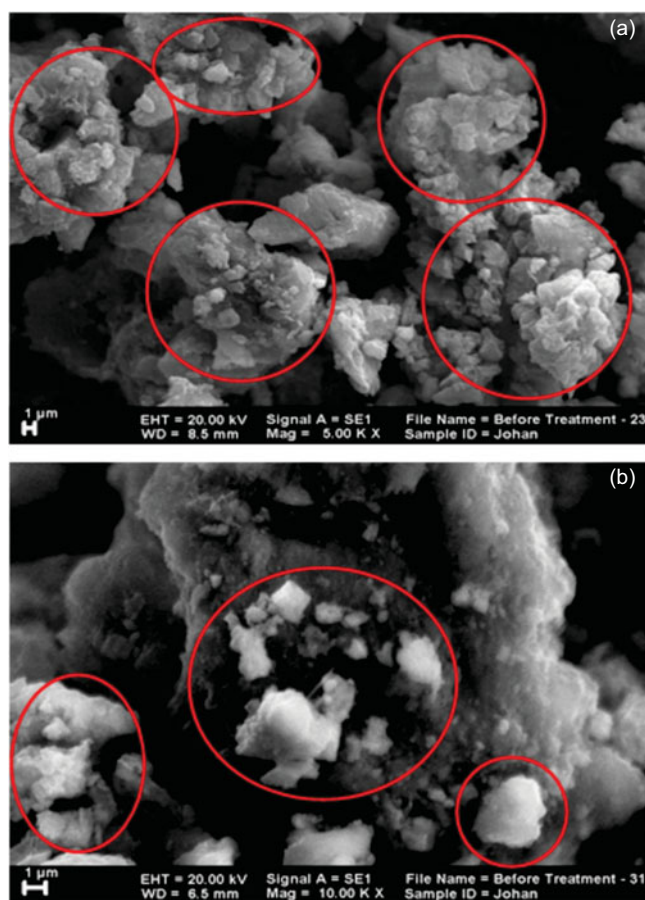
Figure 3. (a) SEM image in the low and magnify times of photocatalyst before used, (O) metal oxides on pore of bentonite. (b) SEM image in the high magnify times of photocatalyst before used, (O) metal oxides on pore of bentonite.
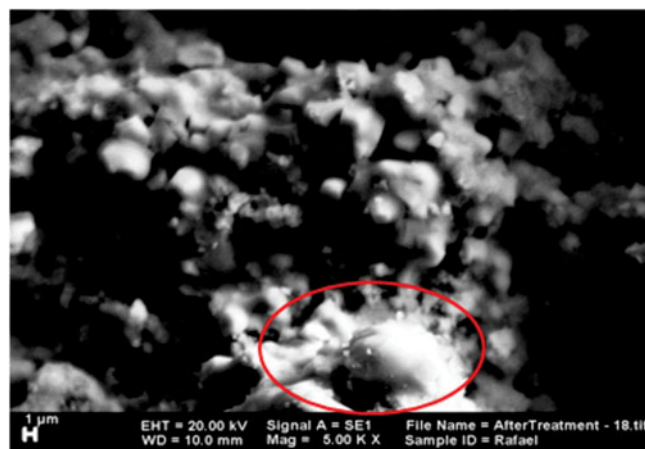
Figure 4. SEM image in the low magnify after treatment, (O) metal oxides on pore of bentonite.

material carried on outflows. This phenomenon is supported by EDX data in Table 1, which shows that amount of Ti and Fe decrease significantly after used in the photocatalytic process.

Moreover, the phenomenon of breaking the bond between the binder and photocatalyst material might be enlightened by the generation of reactive oxygen species (ROS) during the photocatalytic process. The ROS would attack the binder or photocatalyst material and pigment of the paint (Abdulraheem et al., 2012), which causes TiO_2 and Fe_3O_4 break out from the binder and leach with the feed stream. ROS can be marked by the increasing component O in a vessel which is in accordance with the revealed by EDX result. The data demonstrate that the

Table 1. EDX of photocatalyst before and after used in photocatalytic.

Element	% wt (before used)	% wt (after used)
C	5.47	12.41
O	57.1	62.39
Na	0	0.88
Mg	0.14	0.47
Al	1.94	1.46
Si	7.19	3.64
K	0.29	0.28
Ca	17.74	15.71
Ti	1.94	0.8
Fe	8.17	1.96

effectiveness of the photocatalytic material in the photocatalytic process is three times use.

Photocatalytic performance

Effect of dye solution flow rate
Figure 5 shows the effect of dye (Basic Blue 41) solution flow rate ranging from 10, 25, 40, to 65 ml/min, while the other variables were kept constant. Initial dye concentration is 10 ppm and pH of the solution is 5.5 (natural pH of Basic Blue 41).

The result indicated that the decolorization efficiency significantly decreases due to the increase in the dye solution flow rate. The highest efficiency was found to be 97.41% (in 161 min) when the flow rate was maintained at 10 ml/min, while the lowest efficiency was 13.07% (in 30 min) for 65 ml/min dye solution flow rate. Table 2 shows the degradation process efficiency and space-time of dye in the ceramic vessel with different dye solution flow rate.

The dye solution flow rate has a significant role in the continuous system of dye decolorization process. The expected reason is that in high flow rate, the space-time of dye in the ceramics is reduced. Subsequently, the contacting time between dye molecules and photocatalyst particles is reduced. When dye molecule is in contact with photocatalyst particles, the positive hole (h^+) on the TiO_2 material allows it to contact and then react with electron donors in solution. This reaction can generate hydroxyl radicals (OH^*). These radicals would react with adsorbed organic molecules on the surface of the catalyst (Sakka, 2005). The longer the contact time between photocatalyst particles and dye molecules, the more the hydroxyl radicals are formed. Accordingly, there

could be more dye molecules that could be degraded. A lower dye flow rate will result in longer contact time.

Effect of initial dye concentration
Figure 6 shows the effect of initial dye (Basic Blue 41) concentration ranging from 10, 25, 50, 100, to 200 ppm, while the other variables were kept constant. The dye solution flow rate is 10 ml/min, and pH of the solution is 5.5 (natural pH of Basic Blue 41).

As expected, the decolorization efficiency decreases in line with the increase in the dye solution flow rate. The lowest efficiency is found to be 42.26% at the initial dye concentration of 200 ppm, while the highest efficiency is reached at the lowest initial dye concentration.

This phenomenon is related to the number of active sites on the photocatalyst surface. Dye concentration shows the number of dye molecules (substrate) in the solution, whether photocatalyst provides the active sites on its surface as the adsorption sites and space for it to react with dye molecules. The number of active sites on the photocatalyst surface and the number of hydroxyl radicals formed in solution cannot match the number of dye molecules. This causes the contact time between dye molecules and photocatalyst particles to decrease. In addition, the increase in the initial dye concentration could prevent the photocatalyst particles to contact with light, and this result in a decrease in color removal (Abdulraheem et al., 2012). These results proved that the dye solution flow rate has a significant role in the continuous system of dye decolorization process.

Effect of pH
In the photocatalytic process, pH is one of the most important parameters that have an effect on the catalyst particles surface charge and the positions of conductance and valence bands. The previous researcher reported that the optimum pH resulting highest decolorization efficiency is 5.5 (Buyukada, 2016). In this study, the effect of pH on the decolorization process efficiency was also be observed ranging from 3 (acidic condition), 5.5 (natural condition), to 8 (alkaline condition).
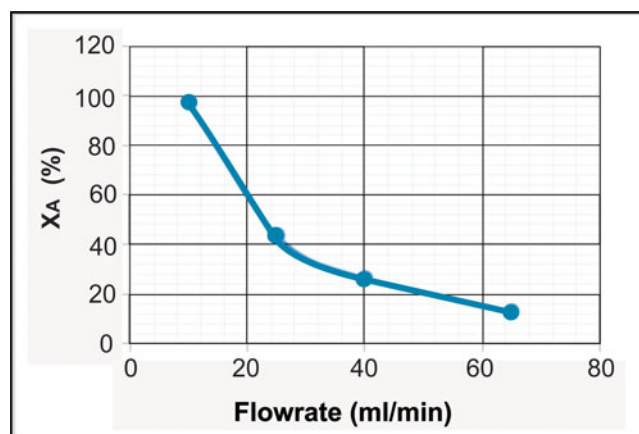
Figure 5. Effect of dye solution flow rate on decolorization of Basic Blue 41 in the presence of bentonite TiO_2–Fe_3O_4 photocatalysts.

Table 2. Decolorization process efficiency and space time of dye with different dye solution flow rate.

Flow rate (ml/min)	Space time (min)	Efficiency (%)
10	161	97.41
25	70	43.74
40	45	26.46
65	30	13.07

The dye solution flow rate is 10 ml/min and dye concentration is 10 ppm.

The charge on the surface of photocatalyst and dye molecules affects the decolorization process as the result of changing the pH solution. This correlation could be explained by the isoelectric point (pH_{IEP}) of dye and point of zero charges of catalyst (pH_{ZPC}). Isoelectric point shows the degree of acidity (pH) when molecule charge is zero due to increasing proton or losing charge in an acid–base reaction. There were three situations to be argued. If solution pH is larger than pH_{IEP} and pH_{ZPC}, a negative repulsive force occurs on dye molecules surface (1), if solution pH is smaller than pH_{IEP} and pH_{ZPC}, a positive repulsive force is occurs (2), and if pH of solution is controlled between pH_{IEP} and pH_{ZPC}, a strong driving force occurs between positive charge of catalyst and negative charge of dye ions (Ciesielczyk et al., 2011). This third condition leads color removal to increase because of the increasing of attraction force between photocatalyst and dye molecules.

Figure 7 shows the highest decolorization process efficiency is at pH 5.5 where this value of pH is between pH_{ZPC} and pH_{IEP}. The pH_{IEP} value of Basic Blue is 3.8 (Ciesielczyk et al., 2011), and the pH_{ZPC} value of TiO_2 and Fe_3O_4 is 6.8 (Abdulraheem, 2012) and 7.9 (Buyukada, 2016). The surface of Basic Blue molecules would be on negative charge condition because the pH of the solution is greater than its pH_{IEP}, while the surface of TiO_2 and Fe_3O_4 particles would be on positive charge condition because the pH of the solution is smaller than their pH_{ZPC}. Bentonite as photocatalyst supporting material contains small positive metal ions on its surface, such as Ca^{2+}, Mg^{2+}, and Na^+. It causes a great attractive force between dye molecules and photocatalyst particles so the adsorption of dye molecules could increase.

At pH value of 3, which is lower than pHIEP and pHZPC, H^+ ions are accumulated on the surface of the photocatalyst. This causes the surface of the photocatalyst and the dye molecule to be positively charged. While at pH value of 8, OH^- ions are accumulated on the surface of the photocatalyst. As the result, the surface to be negatively charged. Both of these cause a great repulsive force between dye molecules and photocatalyst particles so the dye molecules and the photocatalyst particles cannot be adsorbed on the catalyst surface. This result proved that pH of the solution was an important parameter for photocatalytic decolorization process in the continuous system.

Kinetics of photocatalytic decolorization

The kinetics of photocatalytic decolorization has been investigated in the batch system using initial dye concentration of 10 ppm and pH at 5.5.
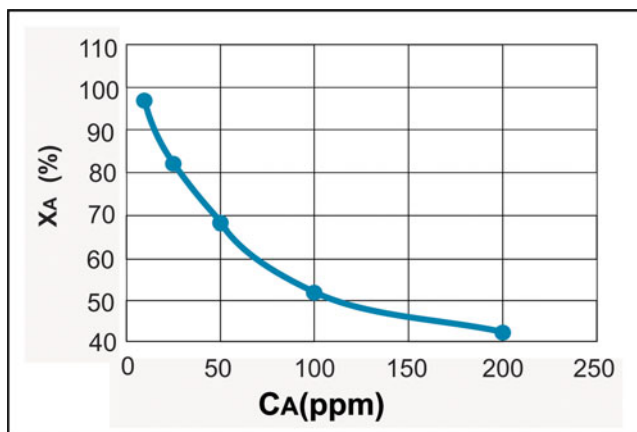
Figure 6. Effect of initial dye concentration on decolorization of Basic Blue 41 in the presence of bentonite TiO_2–Fe_3O_4 photocatalysts.

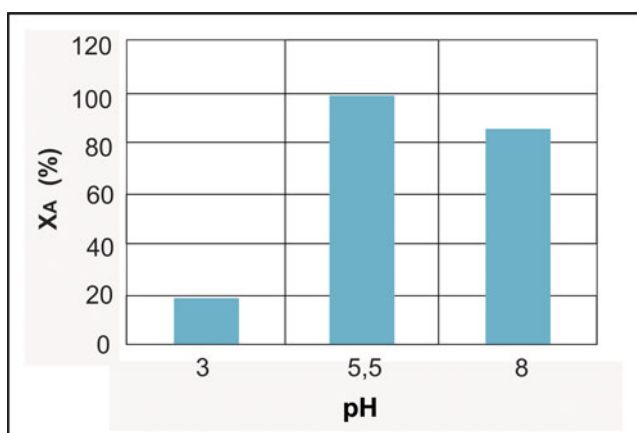**Figure 7.** Effect of pH on decolorization of Basic Blue 41 in the presence of bentonite TiO_2–Fe_3O_4 photocatalysts.

First, the photodegradation of the dye was illustrated by the first-order kinetics model as shown in Equations (2) and (3) (Levenspiel, 2003):

$$-\frac{dC_A}{dt} = kC_A \qquad (2)$$

$$ln\frac{C_{Ao}}{C_A} = kt \qquad (3)$$

where C_{A0} is the initial dye concentration (ppm), C_A is the dye concentration at time t (ppm), t is the time of irradiation (min), and k is the reaction rate constant (min^{-1}).

The data was plotted between linear regression $ln(C_{A0}/C_A)$ versus the time of irradiation to obtain slope which is equal to k based on Equation (3) as shown in Figure 8(a).

The photodegradation of the dye was also illustrated by the second-order kinetics model as shown in Equations (4) and (5) (Levenspiel, 2003):

$$-\frac{dC_A}{dt} = kC_A^2 \qquad (4)$$

$$\frac{1}{C_A} - \frac{1}{C_{Ao}} = kt \qquad (5)$$

where C_{A0} is the initial dye concentration (ppm), C_A is the dye concentration at time t (ppm), t is the irradiation time (min), and k is the reaction rate constant (min^{-1}).

The data was plotted between linear regression $1/C_A$ versus irradiation time to get slope equal to k according to Equation (5) as shown in Figure 9(a).

The first-order kinetic expression can be effectively applied to investigate the decolorization rate in the process. The correlation coefficient, the R^2 value was 0.9812, which designated a very good fitting. Compared to the second-order kinetic, the R^2 value was only 0.7066, which lower than the correlation coefficient of first-order kinetics. Figure 10(b) shows the decrease in the dye concentration of first-order kinetics trend from the
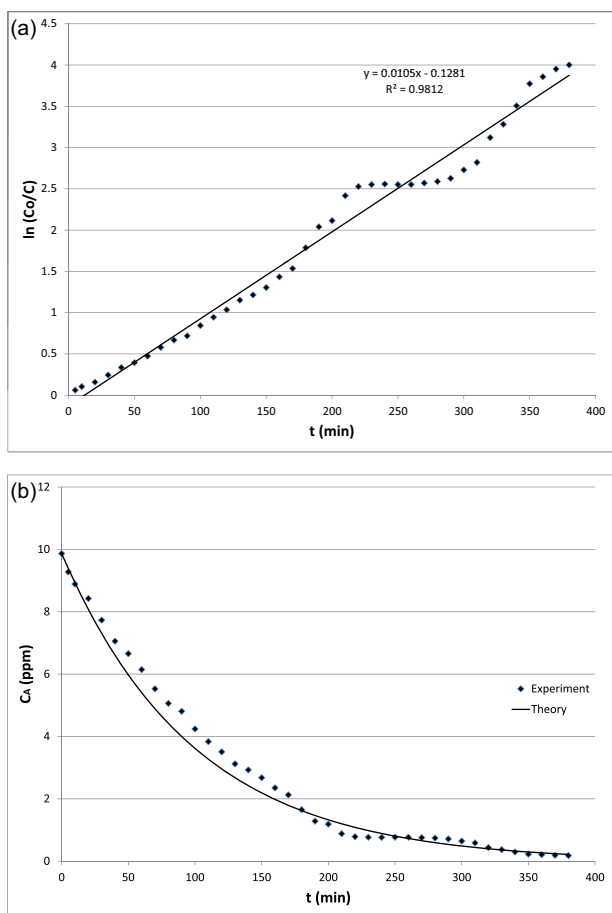
Figure 8. (a) First-order kinetic of photocatalytic decolorization of Basic Blue 41. (b) Decreasing of dye concentration based on first-order kinetic.
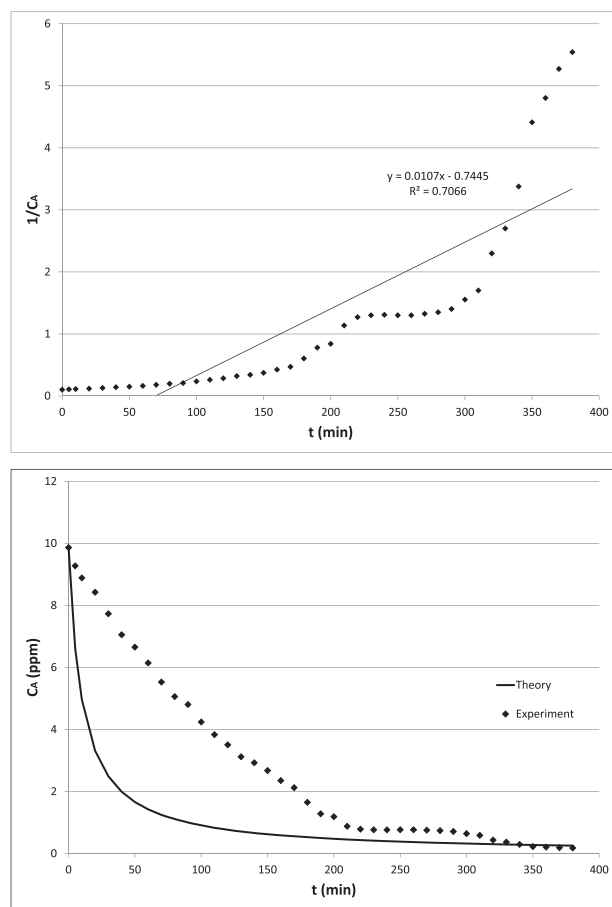

Figure 9. (a) Second-order kinetic of photocatalytic decolorization of Basic Blue 41. (b) Decreasing of dye concentration based on second-order kinetic.
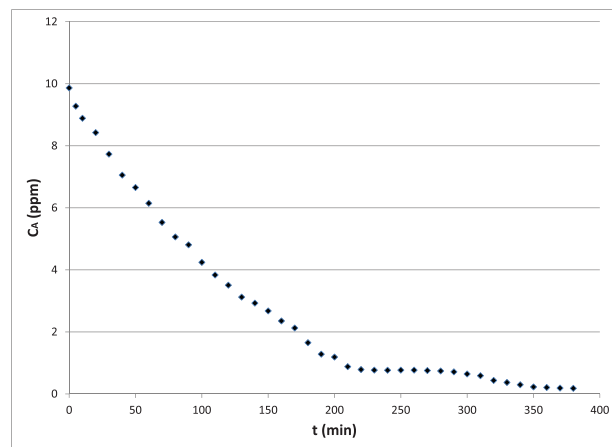
Figure 10. Decreasing of dye concentration (ppm) against time (min) in batch system (using mercury lamp irradiation).

experiment is nearly equal with the decreasing trend from the theory. These results indicated that decolorization rate follows first-order kinetics. The apparent constant rate of Basic Blue decolorization was 0.01 (min^{-1}) at the initial concentration of 10 ppm.

To describe the photocatalytic decolorization process in more detail, Langmuir–Hinshelwood model was used to analyze the adsorption and the reaction constant rate of the photocatalytic process, which took place at the surface of the catalyst, as shown in Equation (6) (Levenspiel, 2003; Sakka, 2005).

$$r = -\frac{dC}{dt} = \frac{k_r.K.C_A}{1 + K.C_A} \tag{6}$$

$$t = \frac{1}{K.k_r}ln\left(\frac{C_{Ao}}{C_A}\right) + \frac{1}{k_r(C_{Ao} - C_A)} \tag{7}$$

$$ln\left(\frac{C_{Ao}}{C_A}\right) + K(C_{Ao} - C_A) = k_r.K.t \tag{8}$$

As explained before, the kinetics of photocatalytic decolorization follows first-order kinetics, where the dye concentration used in the experiment is low. Thus, we can simplify the second term on the right-hand side of Equation (8) to first-order equation as shown in Equation (9) (Sakka, 2005; Levenspiel, 2003):

Figure 11. First-order kinetic for Langmuir–Hinshelwood fit of photocatalytic decolorization of Basic Blue 41.

$$r = -\frac{dC}{dt} = k_r.K.C_A = K_C.C_A \qquad (9)$$

$$ln\left(\frac{C_{Ao}}{C_A}\right) \cong k_r.K.t \cong K_C.t \qquad (10)$$

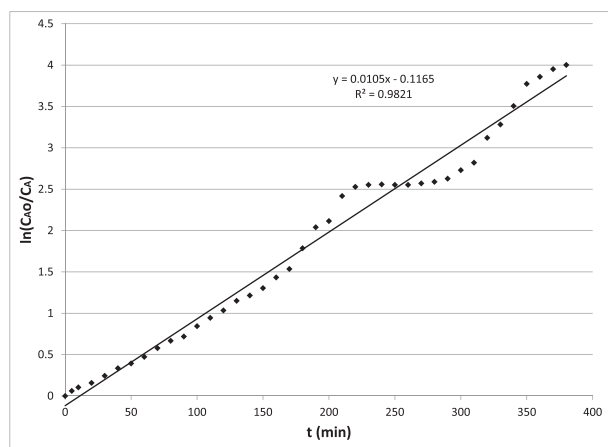where r is the photocatalytic reaction rate (ppm/min), C_{A0} is the initial dye concentration (ppm), C_A is the dye concentration at time t (ppm), t is the irradiation time (min), the k_r is the reaction rate constant, K is the adsorption rate constant, and K_c is the apparent rate constant (min^{-1}).

The data was plotted between linear transforms $ln(C_{A0}/C_A)$ versus irradiation time to get slope equal to K_c according to Equation (10) as shown in Figure 11.

The first-order kinetic expression can be effectively applied to investigate the heterogeneous decolorization reaction of the dye solution, based on our experimental conditions. The value of K_c of Basic Blue 41 decolorization process was 0.01 (min^{-1}) which lead to high efficiency of 98,17% at batch system process. From the intercept, the adsorption rate constant, namely K is obtained with the value of 0.01298, and from the slope, the reaction rate constant, namely k_r is obtained with the value of 0.7707. This data indicated that photo-reaction process between the dye molecules and photocatalyst particles was more dominant than that of the adsorption process of dye molecules onto catalyst surface.

Conclusions

Photocatalyst material of TiO_2-Fe_3O_4-bentonite was successfully synthesized by using the sol–gel method and then to be coated onto ceramic. The material demonstrated ability to degrade of Basic Blue 41 by the photocatalytic process. This study shows that the dye solution can be removed by degradation reaction with high efficiency using the continuous system.

Dye decolorization process in the continuous system is affected by dye solution flow rate, initial dye concentration, and pH of the solution. The flow rate and initial concentration of dye could affect the efficiency where the larger flow rate and initial concentration value, then the efficiency would decrease. The optimum flow rate and initial concentration of dye obtained in this study are 10 ml/min and 10 ppm. The optimum pH of the solution is 5.5 that obtained between pH_{IEP} of dye and pH_{ZPC} of photocatalyst material. At pH 5.5, an attractive force occurs between dye molecules and photocatalyst particles which lead to the increase in the process efficiency. Based on the Langmuir–Hinshelwood kinetic model, it can be revealed that Bentonite TiO_2–Fe_3O_4 is able to act as a good photocatalyst to degrade the Basic Blue 41 under the present experimental conditions.

Disclosure statement

No potential conflict of interest was reported by the authors.

References

Abdulraheem, G., Obinna, N. P., Bello, K. A., and Kolawole, K. A. (2012). Photocatalytic Decolourization and Degradation of C. I. Basic Blue 41 Using TiO_2 Nanoparticles, *J. Environ. Prot.*, **3**, 1063–1069.

Ahmad, R., and Kumar, R. (2010). Adsorption studies of hazardous malachite green onto treated ginger waste, *J. Environ. Manage.*, **91**, 1032–1038.

Ai, L., Huang, H., Chen, Z., Wei, X., and Jiang, J. (2010). Activated carbon/$CoFe_2O_4$ composites: Facile synthesis, magnetic performance and their potential application for the removal of malachite green from water, *Chem. Eng. J.*, **156**, 243–249.

Ameta, R., Surbhi, B., Aarti, A., and Suresh, C. A. (2013). Photocatalytic degradation of organic pollutants: A review, *Mater. Sci. Forum*, **734**, 247–272.

Bhatia, S., Wong, C., and Abdullah, A. (2009). Optimization of air-borne butyl acetate adsorption on dual-function Ag-Y adsorbent-catalyst using response surface methodology, *J. Hazard. Mater.*, **164**, 1110–1117.

Buyukada, M. (2016). Prediction of photocatalytic decolorization and mineralization efficiencies of basic blue 3 using TiO_2 by nonlinear modeling based on box-behnken design, *Arab. J. Sci. Eng.*, **41**, 2631–2646.

Chanathaworn, J., Pornpunyapat, J., and Chungsiriporn, J. (2014). Decolorization of dyeing wastewater in continuous photoreactors using TiO_2 coated glass tube media, *J. Sci. Technol.*, **36**, 97–105.

Chong, M. N., Vimonses, V., Lei, S., Jin, B., Chow, C., and Saint, C. (2009). Synthesis and characterization of novel titania impregnated kaolinite nano-photocatalyst, *Micropor. Mesopor. Mater.*, **117**, 233–242.

Ciesielczyk, F., Nowacka, M., Przybylska, A., and Jesionowski, T. (2011). Dispersive and electrokinetic evaluations of alkoxysilane-modified MgO-SiO$_2$ oxide composite and pigment hybrids supported on it, *Colloids Surf.*, **376**, 21–30.

Djellabi, R., Ghorab, M. F., Cerrato, G., Morandi, S., Gatto, S., Oldani, V., Di Michele, A., and Bianchi, C. L. (2014). Photoactive TiO_2–montmorillonite composite for degradation of organic dyes in water, *J. Photochem. Photobiol. A*, **295**, 57–63.

Don, H., Zeng, G., Tang, L., Fan, C., Zhang, C., He, X., and He, Y. (2015). An overview on limitations of TiO2 -based particles for photocatalytic degradation of organic pollutants and the corresponding countermeasures, *Water Res.*, **79**, 128–146.

Habib, M. A., Ismail, I. M. I., Mahmood, A. J., and Ullah, M. R. (2012). Photocatalytic decolorization of brilliant golden yellow in TiO_2 and ZnO suspensions, *J. Saudi Chem. Soc.*, **16**, 423–429.

Hadjltaief, H. B., Galvez, M. E., Zina, M. B., and Costa, P. (2014). TiO_2/clay as a heterogeneous catalyst in photocatalytic/photochemical oxidation of anionic reactive blue 19, *Arab J. Chem.*, doi:10.1016/j.arabjc.2014.11.006.

Hadjltaief, H. B., Zina, M. B., Galvez, M. E., and Costa, P. (2016). Photocatalytic degradation of methyl green dye in aqueous solution over natural clay-supported ZnO–TiO_2 catalysts, *J. Photochem. Photobiol.*, **315**, 25–33.

Judit, M., László, K., Bazsó, E., Volker, Z., André, R., and Imre,. (2008). Photocatalytic oxidation of organic pollutants on titania–clay composites, *Chemosphere*, **70**, 538–542.

Kameshima, Y., Tamura, Y., Nakajima, A., and Okada, K. (2009). Preparation and properties of TiO_2/montmorillonite composites, *Appl. Clay Sci.*, **45**, 20–23.

Levenspiel, O. (2003). *Chemical reaction engineering*, Wiley, New York.

Liu, J., Li, X., Zuo, S., and Yu, Y. (2007). Preparation and photocatalytic activity of silver and TiO_2 nanoparticles/montmorillonite composite, *Appl. Clay Sci.*, **37**, 275–280.

Mahalakshmi, M., Priya, S.V., Arabindoo, B., Palanichamy, M., and Murugesan, V. (2009). Photocatalytic degradation of aqueous propoxur solution using TiO_2 and Hb zeolite-supported TiO_2, *J. Hazard. Mater.*, **161**, 336–343.

Nakata, K., and Fujishima, A. (2012). TiO_2 photocatalysis: Design and applications, *J. Photochem. Photobiol. C*, **13**, 169–189.

Pignatello, J.J., Oliveros, E., and MacKay, A. (2007). Advanced oxidation processes for organic contaminant destruction based on the Fenton reaction and related chemistry, *J. Environ. Sci. Technol.*, **37**, 273–275.

Sakka, S. (2005). *Handbook of Sol-Gel Science and Technology Processing; Characterization and Applications*, Kluwer Academic Publishers, Dordrecht.

Savitri, E., Widi, R.K., and Budhyantoro, A. (2015). The effect of the calcinations temperature during synthesis of TiO_2-Fe_3O_4-Bentonite as photocatalyst material, *J. Chem. Pharm. Res.*, **7**, 70–75.

Widi, R.K., and Budhyantoro, A. (2014). Catalytic performance of TiO_2-Fe_3O_4 supported bentonite for photocatalytic degradation of phenol, *Inter. J. Appl. Eng. Res.*, **9**, 18753–18758.

Widi, R.K., Budhyantoro, A., and Savitri, E. (2014). Catalytic performance of Al-HDTMA bentonite impregnated Fe on phenol hydroxylation, *Inter. J. Appl. Eng. Res.*, **9**, 7521–7529.

Widi, R. K., Budhyantoro, A., and Savitri, E. (2015). Use of TiO_2-Fe_3O_4 pillared bentonite as photocatalyst in photodegradation of basic blue, *J. Chem. Pharm. Res.*, **7**, 183–188.

Widi, R.K., Budhyantoro, A., and Christianto, A. (2017). Phenol hydroxylation on Al-Fe modified-bentonite: Effect of Fe loading, temperature and reaction time, *IOP Conf. Series: Mater. Sci. Eng.*, **273**, 012007.

Xie Chen, Z.M., and Dai, Y.Z. (2009). Preparation of TiO_2/sepiolite photocatalyst and its application to printing and dyeing wastewater treatment, *Environ. Sci. Technol.*, **32**, 123–127.

Zhang, Q., Chaolin, L., and Ting, L. (2012). Rapid photocatalytic degradation of methylene blue under high photon flux UV irradiation: Characteristics and comparison with routine low photon flux, *Int. J. Photoener.*, **2012**, Article ID 398787.